

BASIC SCIENCE ARTICLE



Venous waveform analysis detects acute right ventricular failure in a rat respiratory arrest model

Ryan J. Lefevre¹✉, Matthew B. Barajas¹, Claudius Balzer¹, Franz J. Baudenbacher², Matthias L. Riess^{1,3,4}, Genevieve Staudt⁵, Antonio Hernandez¹ and Susan S. Eagle¹

© The Author(s), under exclusive licence to the International Pediatric Research Foundation, Inc 2022

BACKGROUND: Peripheral intravenous analysis (PIVA) has been shown to be more sensitive than central venous pressure (CVP) for detecting hemorrhage and volume overload. We hypothesized that PIVA is superior to CVP for detecting right ventricular (RV) failure in a rat model of respiratory arrest.

METHODS: Eight Wistar rats were studied in accordance with the ARRIVE guidelines. CVP, mean arterial pressure (MAP), and PIVA were recorded. Respiratory arrest was achieved with IV Rocuronium. PIVA utilizes Fourier transform to quantify the amplitude of the peripheral venous waveform, expressed as the “f1 amplitude”. RV diameter was measured with transthoracic echocardiography.

RESULTS: RV diameter increased from 0.34 to 0.54 cm during arrest, $p = 0.001$, and returned to 0.33 cm post arrest, $p = 0.97$. There was an increase in f1 amplitude from 0.07 to 0.38 mmHg, $p = 0.01$ and returned to 0.08 mmHg, $p = 1.0$. MAP decreased from 119 to 67 mmHg, $p = 0.004$ and returned to 136 mmHg, $p = 0.50$. There was no significant increase in CVP from 9.3 mmHg at baseline to 10.5 mmHg during respiratory arrest, $p = 0.91$, and recovery to 8.6 mmHg, $p = 0.81$.

CONCLUSIONS: This study highlights the utility of PIVA to detect RV failure in small-caliber vessels, comparable to peripheral veins in the human pediatric population.

Pediatric Research (2023) 93:1539–1545; <https://doi.org/10.1038/s41390-022-02278-3>

IMPACT:

- Right ventricular failure remains a diagnostic challenge, particularly in pediatric patients with small vessel sizes limiting invasive intravascular monitor use.
- Intravenous analysis has shown promise in detecting hypovolemia and volume overload.
- Intravenous analysis successfully detects right ventricular failure in a rat respiratory arrest model.
- Intravenous analysis showed utility despite utilizing small peripheral venous access and therefore may be applicable to a pediatric population.
- Intravenous analysis may be helpful in differentiating various types of shock.

INTRODUCTION

Right ventricular (RV) failure is a known complication in adults and children in the perioperative setting. In the latter, respiratory insufficiency and bronchopulmonary disease account for 20% of all pediatric intraoperative cardiac arrests.¹ Preterm infants have an even further increased risk of perioperative morbidity and mortality following cardiac surgery due to bronchopulmonary dysplasia and respiratory distress syndrome, both of which can lead to RV failure.^{2–4} In addition, acute RV failure occurs following surgical correction of congenital cardiac lesions, including tetralogy of Fallot and atrial or ventricular septal defect closure.^{5,6} The risk of respiratory distress syndrome following congenital cardiac surgery persists even in early term (37–38 weeks' gestation) infants compared to those born at term (>39 weeks' gestation) due to

developmental changes which occur late in pregnancy.⁷ RV failure also occurs in approximately 25% of pediatric patients following orthotopic heart transplantation, mostly secondary to increased pulmonary vascular resistance.^{8,9}

These common perioperative complications underscore the importance of continuous and accurate assessment of RV function in adults and, more so, in pediatric patients following cardiac surgery. However, there are significant limitations with standard and invasive monitoring modalities in the pediatric population.^{10,11} Despite prior studies, which have shown the limitations in both static and trended central venous pressure (CVP) values to detect RV failure, CVP is still often used clinically in pediatric congenital cardiac surgery as a continuous surrogate monitor of RV function.^{12–14} Pulmonary artery catheters are rarely used in the setting of pediatric

¹Department of Anesthesiology, Vanderbilt University Medical Center, 1211 Medical Center Drive, Nashville, TN 37232, USA. ²Department of Biomedical Engineering, Vanderbilt University, 2301 Vanderbilt Place, Nashville, TN 37232, USA. ³Department of Pharmacology, Vanderbilt University, 465 21st Avenue South, Nashville, TN 37240, USA. ⁴Department of Anesthesiology, TVHS VA Medical Center, 1310 24th Avenue South, Nashville, TN 37212, USA. ⁵Department of Anesthesiology, Monroe Carroll Jr Vanderbilt Children's Hospital, 2200 Children's Way, Nashville, TN 37232, USA. ✉email: Ryan.Lefevre@vumc.org

Received: 2 February 2022 Revised: 12 July 2022 Accepted: 9 August 2022
 Published online: 30 August 2022

cardiac surgery due to small patient size and complexity of patient anatomy.^{15,16} Systemic mean arterial pressure (MAP) is often monitored continuously to trigger therapies in order to maintain organ-specific perfusion pressures following cardiac surgery. However, hypotension is not specific to any different type of shock that may occur in the perioperative setting such as cardiogenic shock or hemorrhage. Echocardiography is useful in assessing RV function and is both sensitive and specific for detecting RV dysfunction in pediatric patients.^{10,17,18} Despite these benefits, echocardiography is typically only intermittently performed which limits its usefulness as a screening tool in hospitalized patients. Similarly, other imaging modalities exist to evaluate RV size and function including cardiac computed tomography, cardiac magnetic resonance imaging, and radionuclide ventriculography.^{19,20} These modalities each have unique risks and benefits; however, they all require significant resources and are not used for continuous monitoring.

Peripheral intravenous waveform analysis (PIVA) has shown utility in assessing intravascular volume status. PIVA utilizes spectral analysis of a venous waveform from a standard peripheral IV catheter to quantify the pulsatility in a complex venous signal. The “PIVA f1 peak amplitude” is the magnitude of pulsatility at a frequency corresponding to the HR.

During periods of hypovolemia, the f1 peak amplitude decreases compared to baseline measurements.²¹ Conversely, f1 amplitude significantly increases above baseline values during fluid overload in hospitalized adult patients with decompensated heart failure.²² This correlation between volume status and f1 amplitude is thought to be related to the non-linear pressure–volume relationship of the cardiovascular system. When hypovolemic, small volume changes throughout the cardiac cycle do not cause significant venous pressure changes. In contrast, when hypervolemic, compliance is reduced, and small volume changes will cause increased pulsatility in venous pressure waveforms. This concept is similar and related to “stressed” versus “unstressed” volume, but focuses on the pulsatility present in the venous waveform.²³ This pulsatility is quantitatively measured by the f1 amplitude. Acute RV failure can present similarly to volume overload given congestion of blood in the venous system. Due to this congestion, the f1 amplitude may increase during periods of acute RV failure even without changes in intravascular volume. This form of euvoletic acute RV failure can be seen during periods of hypoxemia and hypercarbia induced by respiratory arrest.

Relative to invasive monitors, PIVA has been found to be superior to CVP and pulmonary arterial pressure (PAP) in detecting hypovolemia due to hemorrhage and retrograde autologous priming prior to cardiopulmonary bypass in adult subjects.²⁴ Similarly, PIVA was shown to be more sensitive and specific than CVP or PAP in detecting volume overload in an adult pig hemorrhage and resuscitation model.²⁵ In previous studies, PIVA measurements were obtained in adult-sized veins cannulated with 20 and 18 g catheters. Adult saphenous veins are approximately three times the diameter of pediatric saphenous veins.^{26,27} There is a void of data demonstrating that PIVA technology can be used in small peripheral vessels, such as in the infant pediatric population, to detect RV failure. It is not known if these small vessels can transmit a venous waveform signal with sufficient detail to allow for the PIVA technique to provide meaningful data. This study deliberately utilizes a small animal model with comparable saphenous vein size as seen in the young pediatric population.²⁸

We hypothesized that PIVA will be more sensitive than CVP for detecting acute RV dysfunction in a rat model of respiratory arrest utilizing small-caliber vessels for waveform measurement.

MATERIALS AND METHODS

This study was approved by the Institutional Animal Care and Use Committee at Vanderbilt University Medical Center, Nashville, Tennessee and was carried out and reported in accordance with the ARRIVE

guidelines for animal research (Approval M1800029-00). Ten male Wistar rats 37.2 weeks old (standard deviation [SD] = 1.7) and weighing 423 g (SD = 40) were housed under a 12 h/12 h light/dark cycle with water and food ad libitum. Immediately prior to the experiment, rats were anesthetized with intraperitoneal pentobarbital injection (45 mg kg⁻¹, Diamondback Drugs, Scottsdale, AZ). Rats were intubated with a 14 g angiocatheter²⁹ and mechanically ventilated with 6 mL kg⁻¹ tidal volume, 60 breaths per minute, 50% oxygen in nitrogen mixture (rodent ventilator model 683, Harvard Apparatus, MA). IV pentobarbital was titrated to effect for maintenance of anesthesia. End-tidal CO₂ (EtCO₂) and respiratory rate (RR) were measured by an infrared CO₂-Sensor (Capnogard, Novamatrix, CT). A rectal temperature probe was placed, and the core temperature was maintained constant between 36.5 and 37.5 °C. Electrocardiogram (ECG) was derived from subcutaneous ECG needles to calculate heart rate (HR). Vascular access was established via surgical cut-down using 22 g 1” angiocatheters (Smiths Medical, Minneapolis, MN) in the saphenous vein as well as blunt needles (Air-Tite, Virginia Beach, VA) connected to 25 cm PE tubing (PE25 Instech, Plymouth Meeting, PA) in the femoral artery and internal jugular vein, respectively. A TruWave pressure transducer (Edwards Lifesciences, Irvine, CA) was connected directly to each catheter. ECG, CVP, MAP, and saphenous venous waveforms were recorded using Powerlab Series 16/30 and LabChart Version 8.1.13 (AD Instruments, Dunedin, New Zealand). Respiratory arrest was achieved by IV injection of Rocuronium (3 mg kg⁻¹, Hospira, Lake Forest, IL) and discontinuation of ventilation. Ventilation was held for 8 min. Respiratory arrest was defined as an absence of respiratory effort and an absence of EtCO₂. This asphyxia arrest is typically described as an animal model of biventricular failure and cardiac arrest occurring within 3–4 min after cessation of ventilation.^{30–32} Cardiac arrest was defined by an absence of pulsatility on the arterial pressure tracing despite continued electrical activity on ECG (Pulseless Electrical Activity [PEA] arrest). At the conclusion of the apneic period of 8 min, ventilation was resumed (6 mL kg⁻¹ tidal volume, 60 breaths per minute, 100% inspired oxygen concentration). Intravenous epinephrine was administered (0.01 mg kg⁻¹, Hospira). Chest compressions were performed to a depth of 2 cm and a compression rate of 200 min⁻¹ utilizing a custom-built piston compression device until a systolic blood pressure of 120 mmHg was achieved. When this was achieved, compressions were stopped to evaluate for return of spontaneous circulation (ROSC). ROSC was defined by the return of pulsatility on the arterial pressure tracing and maintenance of EtCO₂ > 20 mmHg in the absence of chest compressions. Ventilation continued, and vital signs were allowed to stabilize after achieving ROSC. An independent experienced echocardiographer obtained and analyzed transthoracic echocardiographic images using an Affiniti 50 C ultrasound with an S12-4 (12–4 MHz frequency range) transducer (Philips Healthcare, Andover, MA); analyses were confirmed by a second independent, experienced echocardiographer. Since RV diameter reliably increases with the development of RV failure in rat species, this study utilizes RV diameter as a marker for RV failure.³³ RV base diameter at end-diastole was measured from an apical 4-chamber view. An RV diameter of >4.5 mm was defined as RV dilation based on a prior rat model of pulmonary hypertension, and this value was used as a marker of RV failure.³³ Superimposed color flow Doppler was also used in this view to assess for tricuspid regurgitation. Left ventricular (LV) ejection fraction (EF) was measured in the parasternal short axis view utilizing the Teicholz method with an EF > 55% considered normal.^{34,35} All measurements were obtained at baseline immediately prior to the initiation of arrest, after 2 min of respiratory arrest, and post ROSC after vital signs stabilized 10–20 min after resuming ventilation.

Venous pressure waveform was analyzed offline after the conclusion of the experiment using a fast Fourier transform (FFT) with an 8 K sampling window with no window overlap. Data were recorded at a sampling rate of 1 kHz necessitating 8 s of continuous time-domain signal to perform the 8K-FFT spectral analysis. The FFT converts the time-domain waveform into a frequency domain output with distinct peaks at a variety of frequencies. These peaks correspond to various physiologic parameters that influence the waveform such as RR and HR. The amplitude of each frequency peak was calculated in LabChart (Fig. 3). The peak amplitude at a frequency corresponding to the HR was labeled f1 (the fundamental frequency). Data were captured in triplicate for each point used in the analysis. To analyze the data, Stata (Stata/IC 16.1, StataCorp LLC, College Station, TX) was used. To ensure normal distribution, a Shapiro–Wilk normality test was run. Normally distributed data were then analyzed using a repeated-measures ANOVA while Kruskal–Wallis H-test was used for non-parametric analysis. Pairwise

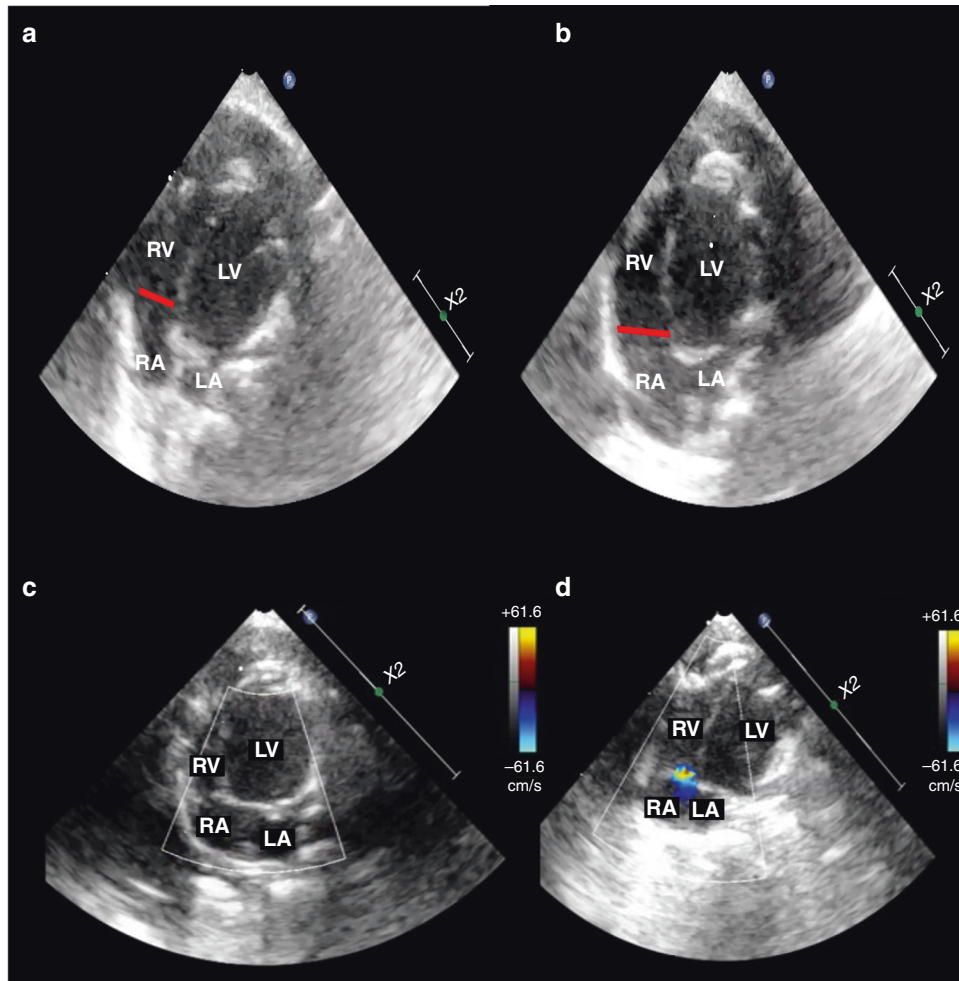


Fig. 1 Echocardiography confirms right ventricular dilation. Representative apical 4-chamber image of end-diastolic RV base diameter (red bar) shown at a normal diameter at baseline (a) and acute RV base dilation during respiratory arrest (b). Superimposed color flow Doppler was used during systole showing no tricuspid regurgitation at baseline (c) and the presence of tricuspid regurgitation during respiratory arrest (d). RV right ventricle, RA right atrium, LV left ventricle, LA left atrium.

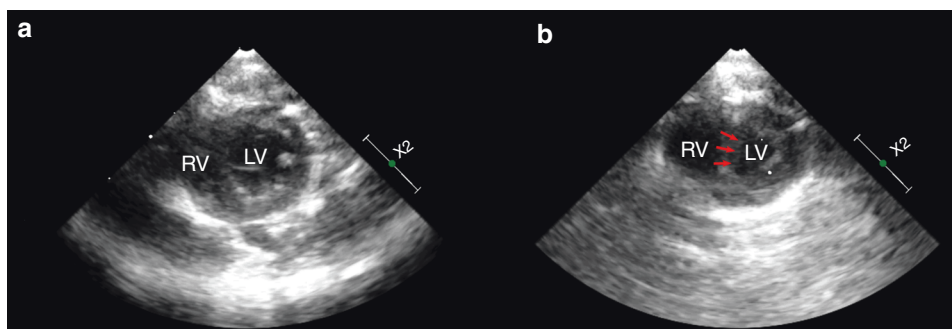


Fig. 2 Echocardiography confirms right ventricular dilation and ventricular septal shift. Representative parasternal short axis images at end-diastole. Baseline (a) shows normal RV and LV size with normal ventricular septum. During respiratory arrest (b), RV dilation can be seen with a D-shaped LV with flattening of the ventricular septum (arrows). RV right ventricle, LV left ventricle.

comparisons were made with Tukey's tests for parametric and Dunn's tests for non-parametric analysis and adjusted per Bonferroni correction. HR and f1 amplitudes were non-normally distributed at a minimum of one timepoint, thus non-parametric tests were performed on these variables, and data were reported as median and inter-quartile range (IQR). A p value <0.05 was considered significant (two-sided). For $\alpha = 0.05$ and a power of 80%, we calculated a sample size of at least seven animals to demonstrate an increase in the f1 amplitude by 50%, assuming a SD of 0.1 based on previous data evaluating f1 amplitude measurements.^{21,22,24,36}

RESULTS

Ten Wistar rats were initially included in the experiment and successfully underwent respiratory arrest leading to PEA cardiac arrest. All rats received IV epinephrine and chest compressions and successfully obtained ROSC. Two rats were subsequently excluded due to malfunction of the pressure transducers leading to inadequate venous waveform recordings. The remaining eight rats successfully completed the experiment and were included in the

analysis. Satisfactory short axis and apical 4-chamber echocardiographic images were obtained in all rats. RV failure occurred in all rats during respiratory arrest, confirmed by significant increases in RV diameter (Fig. 1a, b) and new tricuspid regurgitation (Fig. 1c, d). Subjective RV systolic function as evaluated by two independent, experienced echocardiographers for each rat was described as normal at baseline, severe RV systolic dysfunction during respiratory arrest, and returned to baseline after recovery. LV EF for each rat remained normal and without statistically significant difference at each measurement point (baseline = 60% [SD = 4], arrest = 67%

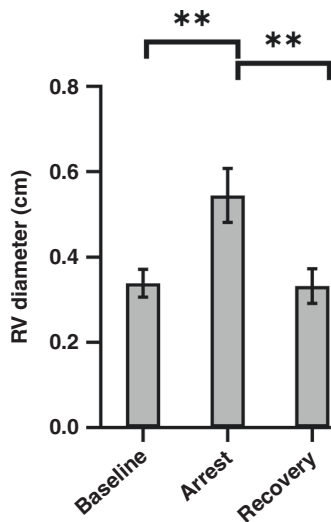


Fig. 3 RV diameter changes with respiratory arrest. End-diastolic RV base diameter increased from a mean of 0.34 cm (SD = 0.03) at baseline to 0.54 cm (SD = 0.06) during respiratory arrest, $p = 0.001$. Post arrest, RV diameter returned to near baseline values, 0.33 cm (SD = 0.04), $p = 0.97$ (vs baseline). ** $p < 0.01$. RV right ventricle.

[SD = 3], post arrest = 63% [SD = 4]) ($p = 0.08$). The LVs in all rats were described as severely underfilled with leftward ventricular septal shift during respiratory arrest (Fig. 2).

The mean RV base diameter increased from 0.34 cm (SD = 0.03) at baseline to 0.54 cm (SD = 0.06) during arrest, $p = 0.001$; post arrest, RV diameter returned to near baseline values, 0.33 cm (SD = 0.04), $p = 0.97$ (vs baseline) (Fig. 3).

Peripheral venous waveforms and FFT (f1 amplitude) corresponding to the subjects' HR measured by ECG were measured at baseline and during respiratory arrest (Fig. 4, representative images).

Peak f1 amplitude significantly increased from a median of 0.07 mmHg (IQR = 0.06–0.23) to 0.38 mmHg (IQR = 0.21–0.49), $p = 0.01$, during respiratory arrest (Fig. 5a). After recovery from respiratory arrest, the f1 amplitude returned from the elevated level during arrest to near baseline levels 0.08 mmHg (IQR = 0.04–0.23), $p = 1.0$ (vs baseline). CVP did not change significantly from baseline, mean 9.3 mmHg (SD = 6.0), to arrest 10.5 mmHg (SD = 4.8) or after recovery from arrest 8.6 mmHg (SD = 3.6), $p = 0.91$ and 0.81, respectively (Fig. 5b). MAP showed a significant decrease during respiratory arrest from 119 mmHg (SD = 23) to 67 mmHg (SD = 22), $p = 0.004$, then recovered to back to baseline values at 136 mmHg (SD = 33) after resumption of ventilation and resuscitation, $p = 0.50$ (vs baseline) (Fig. 5c). HR decreased from a median of 341 beats per minute (bpm) (IQR = 297–379) to 129 bpm (IQR = 114–220), $p = 0.0004$ during respiratory arrest. HR was obtained from ECG which allowed measurement of an HR even during PEA arrest. Recovery HR was slightly lower than baseline at 285 bpm (IQR = 275–318), but was statistically indistinguishable from baseline, $p = 0.18$ (Fig. 5d).

To evaluate diagnostic utility for RV failure, receiver operator characteristic (ROC) curves were constructed and areas under the curve (AUC) compared between all variables (Fig. 6).^{37,38} Notably, the AUC of f1 0.91 (SD = 0.08) was significantly higher than that of CVP 0.57 (SD = 0.15), $p = 0.04$. However, the f1 AUC did not differ from that of MAP 0.95 (SD = 0.05) or HR 0.92 (SD = 0.08), $p = 0.57$ and $p = 0.85$, respectively. Both MAP and HR AUCs were significantly

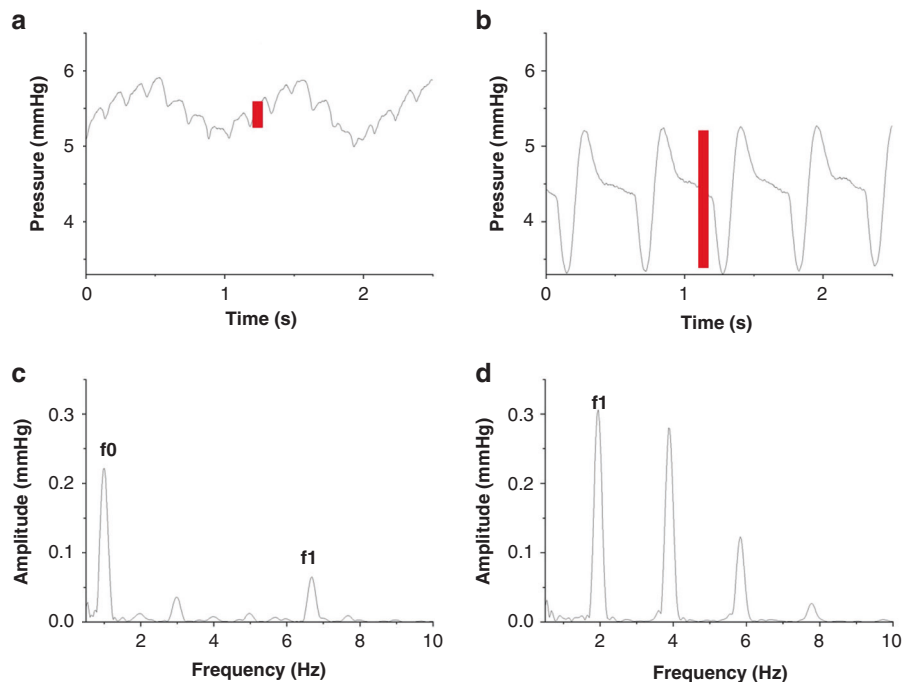


Fig. 4 Venous waveform changes during respiratory arrest. Representative venous waveform shown at baseline (a) and during respiratory arrest (b). Corresponding changes in spectral analysis shown at baseline (HR 405 bpm = 6.75 Hz) (c) and during respiratory arrest (HR 120 bpm = 2 Hz) resulting in d a significant increase in f1 amplitude. This f1 peak represents a quantitative measure of the pulsatility in the venous waveform signal (red bars). The f0 peak on the baseline spectral analysis occurs at a frequency corresponding to the respiratory rate and is therefore not present on the respiratory arrest spectral analysis. HR heart rate, bpm beats per minute.

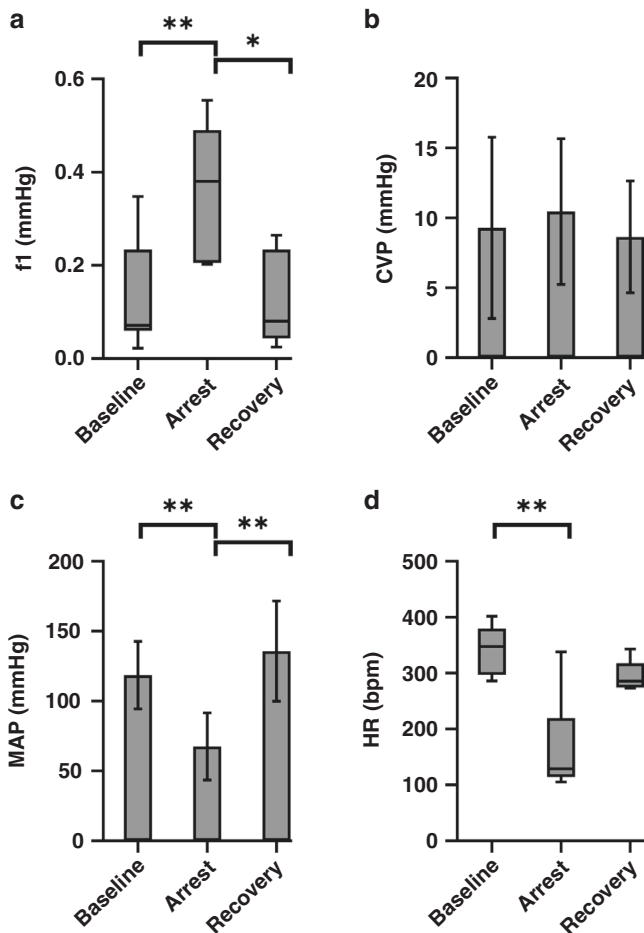


Fig. 5 Hemodynamic changes with respiratory arrest. **a** PIVA f1 amplitude from a saphenous venous waveform increased from 0.07 mmHg (IQR = 0.06–0.23) to 0.38 mmHg (IQR = 0.21–0.49), $p = 0.01$, during respiratory arrest. After recovery from respiratory arrest, the f1 amplitude returned to near baseline levels 0.08 mmHg (IQR = 0.04–0.23), $p = 1.0$ (vs baseline). $*p < 0.05$, $**p < 0.01$. **b** CVP did not change significantly from baseline 9.3 mmHg (SD = 6.0) during arrest 10.5 mmHg (SD = 4.8) nor after recovery from arrest 8.6 mmHg (SD = 3.6), $p = 0.91$ and 0.81, respectively. **c** MAP significantly decreased during respiratory arrest from 119 mmHg (SD = 23) to 67 mmHg (SD = 22), $p = 0.004$, then recovered to near baseline values at 136 mmHg (SD = 33), $p = 0.5$ (vs baseline). $**p < 0.01$. **d** HR decreased during respiratory arrest from 341 bpm (IQR = 297–379) at baseline to 129 bpm (IQR = 114–220), $p = 0.0004$. Recovery HR at 285 bpm (IQR = 275–318) was statistically indistinguishable from baseline, $p = 0.18$. $**p < 0.01$. PIVA peripheral intravenous waveform analysis, CVP central venous pressure, MAP mean arterial pressure, HR heart rate, bpm beats per minute.

higher than that of CVP, $p = 0.01$ and $p = 0.02$, respectively, but did not differ from each other, $p = 0.68$.

DISCUSSION

In this study, we investigated the utility of PIVA to detect RV dysfunction using a rat model of respiratory arrest and resuscitation. In contrast to prior studies evaluating a decrease in f1 amplitude in the setting of hypovolemia, this study shows that increases in PIVA signal may be a both sensitive and specific method to detect isolated RV failure, particularly in the setting of respiratory insufficiency in the perioperative setting. There are several advantages to this method that can be translated to the human pediatric population. First, PIVA uses a peripheral IV, which

is standard for pediatric patients in the perioperative setting. The animals used had similarly sized saphenous veins to neonatal and young infant patients. While previous PIVA studies were performed in large adult animals and humans, it was not known if small-caliber vessels would transmit a venous waveform from which meaningful data could be derived. Thus, this is the first study that demonstrates that the PIVA signal can accurately detect heart failure in small peripheral vessels, such as seen in infant pediatric populations. Furthermore, this is the first study that associates a significant increase in the PIVA signal with RV failure assessed by echocardiography.

In this study, there were no statistically significant changes in CVP even during severe RV failure and ultimately cardiovascular collapse. These results indicate that, in contrast to pure CVP, PIVA is a highly promising monitoring modality in high-risk pediatric patients presenting for surgery, specifically in the newborn and very premature population where respiratory compromise and RV failure are problematic.

Furthermore, PIVA was shown to decrease toward baseline after ROSC and improvement of RV function. This information may be useful in cardiac surgery and postoperative settings for treating RV failure using inotropic support.

Each rat in this study became hypotensive during the respiratory arrest. PIVA, in fact, was not superior to MAP in detecting RV failure. However, while all types of shock may present with hypotension, the treatment algorithms for each type are very different. Thus, the etiology of hypotension must be rapidly elucidated. In contrast to prior studies which showed a decrease in the PIVA f1 amplitude with hemorrhage, this study demonstrated an increase in the PIVA f1 amplitude with RV failure. Thus, PIVA distinguishes between two common types of hypotension and shock in the perioperative setting: hemorrhage vs cardiac (RV) failure. This combination of sensitivity and specificity may make PIVA a very useful tool for the rapid assessment and management of acute hypotension in the perioperative setting. Additional studies are needed to assess the PIVA signal during LV or biventricular failure. Similar to MAP, HR also decreased significantly during the respiratory arrest. Much like MAP, a decrease in HR is not specific in differentiating various forms of shock. While changes in HR can be used as a clinical indicator of a potentially acute cardiopulmonary event, changes in f1 amplitude provide a more granular distinction between shock states, such as hypovolemia and heart failure, for rapid and accurate treatment decisions. It is not known if the changes in HR itself might affect the f1 amplitude measurement, and future studies are planned to clarify this relationship.

The results of this study should be evaluated within its natural constraints. Although it achieved statistical significance, the sample size was small in this feasibility study, and AUC values need to be interpreted with caution. Larger studies are needed to confirm that these findings remain consistent. The study was also performed on a rat model of RV failure. Prior studies have shown a good translation of the utility of PIVA between small animals, large animals, and humans when detecting hypovolemia. Future studies will aim at examining RV failure in pediatric subjects.

RV failure was obtained with the cessation of ventilation. Our study produced similar results to previous studies with PEA cardiac arrest developing within 3–4 min. The study data was taken 2 min after cessation of ventilation when RV failure had occurred, but LV function was preserved. Given that this technique depends on quantifying pulsatility in the cardiovascular system, the authors suspect it would not provide utility later into the arrest period with absent pulsatility. It is unknown if CPR alone would provide sufficient pulsatility to draw meaningful conclusions. While hypoxemia and hypercarbia are certainly common causes of RV failure, alternative etiologies include myocardial ischemia, volume overload, pulmonary embolism, and sepsis. In addition,

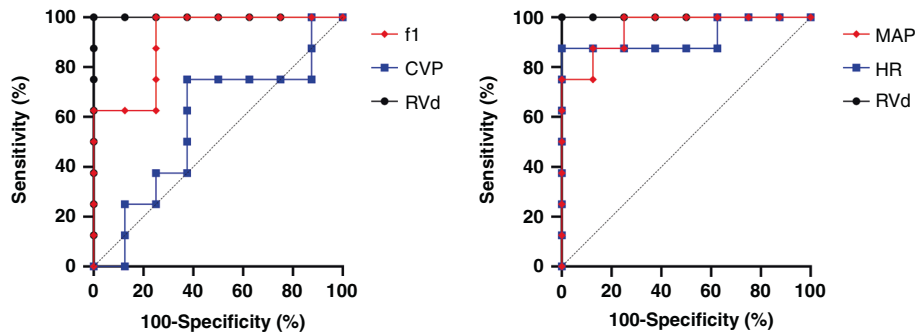


Fig. 6 Receiver operator characteristic curve for detection of RV failure. f1 and CVP ROC curves are displayed on the left, and MAP and HR ROC curves are displayed on the right, both compared to echo-assessed standard of RV diameter. f1 AUC 0.91 (SD = 0.08) was significantly higher than that of CVP 0.57 (SD = 0.15), $p = 0.04$ but did not differ from MAP 0.95 (SD = 0.05) or HR 0.92 (SD = 0.08), $p = 0.57$ and $p = 0.85$, respectively. Both MAP and HR AUC were significantly higher than CVP, $p = 0.01$ and $p = 0.02$, respectively, but did not differ from each other, $p = 0.68$. AUC area under the curve, CVP central venous pressure, MAP mean arterial pressure, HR heart rate, RVd right ventricular diameter, ROC receiver operator characteristic.

the RV failure in this study was acute, and the rats recovered their RV function after resuming ventilation. This model most closely represents acute respiratory failure. Clinically, RV failure can be chronic, and it is not known if the demonstrated changes in the PIVA f1 amplitude persist in that setting. Further studies are needed to evaluate this technique across a heterogeneous population with other causes of RV failure.

While we expect that the venous waveform signal would be more sensitive to right-sided cardiac dysfunction, more data is needed to determine the effect of congenital heart disorders including single ventricular function in patients with Fontan physiology on PIVA. More data is also needed to determine the effects of various pharmacologic agents, such as different vasoactive agents on the PIVA signal.

Venous waveforms were obtained from a proximal saphenous vein in this study, as this was the most distal vessel that produced a reliable venous signal in a rat model. The saphenous vein is frequently cannulated in pediatric patients and, thus, has great utility for use in perioperative monitoring. Further studies are needed to determine the effects of different venous cannulation sites, such as upper extremity or external jugular veins, on the PIVA signal in pediatric patients. Furthermore, only male rats were used in this study. Additional studies using female rats are warranted as the vessel diameter may be smaller than in the male counterpart.

Transthoracic echocardiography was used to measure end-diastolic RV base diameter to confirm the diagnosis of RV failure. RV function can also be assessed with echocardiography by several other techniques including, but not limited to, fractional area change, tricuspid annular plane systolic excursion (TAPSE), and visual estimation. The rats experienced cardiovascular decompensation quickly with respiratory arrest, so performing the measurements quickly was critical to ensure timing remained consistent for all rats. Thus, RV base diameter was selected for this study due to the ease in obtaining a consistent view needed to perform the measurement quickly. In the authors' experience, measurements such as TAPSE and fractional area change take more time to perform accurately in rats, which could interfere with study timing. Nonetheless, RV dilation is only one assessment of RV function: RV systolic dysfunction can occur without RV dilation, and conversely, RV dilation can occur without systolic dysfunction. Additional models are needed where RV failure occurs more slowly allowing a more thorough evaluation of RV dysfunction along with PIVA.

All rats received pentobarbital for maintenance of anesthesia. Pentobarbital has been associated with hemodynamic changes such as a decrease in HR and MAP; however, it is not known what effect, if any, these changes have on PIVA waveforms. Further

studies are needed with a variety of anesthetic agents to determine their effects on PIVA waveforms.

Two rats were excluded from this study. The pressure monitor used to record the venous waveforms malfunctioned and thus adequate waveforms could not be recorded. Of note, these two experiments occurred on consecutive days, and after identification and replacement of the malfunctioning equipment, no further malfunctions were encountered. Nonetheless, given that this technique strongly depends on the analysis of venous waveforms, these temporary failures show that PIVA does require appropriately functioning IV catheters and monitors to provide meaningful information.

CONCLUSIONS

PIVA is both sensitive and specific for acute RV failure and recovery in a rat model of pediatric respiratory arrest and resuscitation. PIVA was superior to CVP in detecting RV failure. While PIVA was not superior to MAP in detecting RV failure, it may be more clinically useful than MAP in the ability of PIVA to distinguish between acute RV failure and other types of shock. Based on the results of this study, we plan to continue to investigate PIVA as an effective continuous monitor to detect RV failure. Future studies will be translated clinically to pediatric subjects in order to validate the technique in the perioperative and critical care setting.

DATA AVAILABILITY

The datasets generated during and/or analyzed during the current study are available from the corresponding author on reasonable request.

REFERENCES

- Murray, J. P. et al. Anesthesia-related cardiac arrest in children: initial findings of the Pediatric Perioperative Cardiac Arrest (POCA) Registry. *Anesthesiology* **93**, 6–14 (2000).
- McMahon, C. J. et al. Preterm infants with congenital heart disease and bronchopulmonary dysplasia: postoperative course and outcome after cardiac surgery. *Pediatrics* **116**, 423–430 (2005).
- Cheung, P. Y. et al. Outcomes of preterm infants with congenital heart defects after early surgery: defining risk factors at different time points during hospitalization. *Front. Pediatr.* **8**, 616659 (2020).
- Altit, G., Bhombal, S., Feinstein, J., Hopper, R. K. & Tacy, T. A. Diminished right ventricular function at diagnosis of pulmonary hypertension is associated with mortality in bronchopulmonary dysplasia. *Pulm. Circ.* **9**, 2045894019878598 (2019).
- de Boer, J. M., Kuipers, I. M., Klitsie, L. M., Blom, N. A. & Ten Harkel, A. D. Decreased biventricular longitudinal strain shortly after congenital heart defect surgery. *Echocardiography* **34**, 446–452 (2017).

6. Pauliks, L. B., Valdes-Cruz, L. M., Perryman, R. & Scholl, F. G. Right ventricular wall-motion changes after infant open heart surgery—a Tissue Doppler Study. *Echocardiography* **31**, 209–217 (2014).
7. Costello, J. M. et al. Gestational age at birth and outcomes after neonatal cardiac surgery: an analysis of the Society of Thoracic Surgeons Congenital Heart Surgery Database. *Circulation* **129**, 2511–2517 (2014).
8. Hoskote, A. et al. Acute right ventricular failure after pediatric cardiac transplant: predictors and long-term outcome in current era of transplantation medicine. *J. Thorac. Cardiovasc. Surg.* **139**, 146–153 (2010).
9. Ofori-Amanfo, G. et al. Heart transplantation in children with markedly elevated pulmonary vascular resistance: impact of right ventricular failure on outcome. *J. Heart Lung. Transpl.* **30**, 659–666 (2011).
10. Lopez, L. et al. Recommendations for quantification methods during the performance of a pediatric echocardiogram: a report from the Pediatric Measurements Writing Group of the American Society of Echocardiography Pediatric and Congenital Heart Disease Council. *J. Am. Soc. Echocardiogr.* **23**, 465–495 (2010).
11. Skowno, J. J. & Broadhead, M. Cardiac output measurement in pediatric anesthesia. *Paediatr. Anaesth.* **18**, 1019–1028 (2008).
12. Marik, P. E. & Cavallazzi, R. Does the central venous pressure predict fluid responsiveness? An updated meta-analysis and a plea for some common sense. *Crit. Care Med.* **41**, 1774–1781 (2013).
13. Renner, J. et al. Prediction of fluid responsiveness in infants and neonates undergoing congenital heart surgery. *Br. J. Anaesth.* **108**, 108–115 (2012).
14. Gan, H., Cannesson, M., Chandler, J. R. & Ansermino, J. M. Predicting fluid responsiveness in children: a systematic review. *Anesth. Analg.* **117**, 1380–1392 (2013).
15. Singh, Y. et al. Recommendations for hemodynamic monitoring for critically ill children—expert consensus statement issued by the Cardiovascular Dynamics Section of the European Society of Paediatric and Neonatal Intensive Care (Espnic). *Crit. Care* **24**, 620 (2020).
16. American Society of Anesthesiologists Task Force on Pulmonary Artery Catheterization. Practice guidelines for pulmonary artery catheterization: an updated report by the American Society of Anesthesiologists Task Force on Pulmonary Artery Catheterization. *Anesthesiology* **99**, 988–1014 (2003).
17. Frommelt, P. C., Ballweg, J. A., Whitstone, B. N. & Frommelt, M. A. Usefulness of Doppler tissue imaging analysis of tricuspid annular motion for determination of right ventricular function in normal infants and children. *Am. J. Cardiol.* **89**, 610–613 (2002).
18. van der Zwaan, H. B. et al. Clinical value of real-time three-dimensional echocardiography for right ventricular quantification in congenital heart disease: validation with cardiac magnetic resonance imaging. *J. Am. Soc. Echocardiogr.* **23**, 134–140 (2010).
19. Mooij, C. F., de Wit, C. J., Graham, D. A., Powell, A. J. & Geva, T. Reproducibility of MRI measurements of right ventricular size and function in patients with normal and dilated ventricles. *J. Magn. Reson. Imaging* **28**, 67–73 (2008).
20. Leibundgut, G. et al. Dynamic assessment of right ventricular volumes and function by real-time three-dimensional echocardiography: a comparison study with magnetic resonance imaging in 100 adult patients. *J. Am. Soc. Echocardiogr.* **23**, 116–126 (2010).
21. Lefevre, R. J. et al. Venous waveform analysis correlates with echocardiography in detecting hypovolemia in a rat hemorrhage model. *Semin. Cardiothorac. Vasc. Anesth.* **25**, 11–18 (2021).
22. Miles, M. et al. Peripheral intravenous volume analysis (PIVA) for quantitating volume overload in patients hospitalized with acute decompensated heart failure—a pilot study. *J. Card. Fail.* **24**, 525–532 (2018).
23. Spiegel, R. Stressed vs. unstressed volume and its relevance to critical care practitioners. *Clin. Exp. Emerg. Med.* **3**, 52–54 (2016).
24. Sileshi, B. et al. Peripheral venous waveform analysis for detecting early hemorrhage: a pilot study. *Intensive Care Med.* **41**, 1147–1148 (2015).
25. Hocking, K. M. et al. Peripheral venous waveform analysis for detecting hemorrhage and iatrogenic volume overload in a porcine model. *Shock* **46**, 447–452 (2016).
26. Cole, I., Glass, C., Norton, H. J. & Tayal, V. Ultrasound measurements of the saphenous vein in the pediatric emergency department population with comparison to I.V. catheter size. *J. Emerg. Med.* **43**, 87–92 (2012).
27. Kim, M. J. et al. Association between venous reflux and diameter of great saphenous vein in lower thigh. *J. Vasc. Surg. Venous Lymphat. Disord.* **8**, 100–105 (2020).
28. Lóránt, M., Nádas, G. L., Raffai, G. & Monos, E. Remodeling of the rat saphenous vein network in response to long-term gravitational load. *Physiol. Res.* **52**, 525–531 (2003).
29. Balzer, C., Cleveland, W. J., Jinka, T. R. & Riess, M. L. Video laryngoscopic oral intubation in rats: a simple and effective method. *Am. J. Physiol. Lung Cell Mol. Physiol.* **318**, L1032–L1035 (2020).
30. Katz, L., Ebmeyer, U., Safar, P., Radovsky, A. & Neumar, R. Outcome model of asphyxial cardiac arrest in rats. *J. Cereb. Blood Flow. Metab.* **15**, 1032–1039 (1995).
31. Ebmeyer, U., Keilhoff, G. & Wolf, G. [The asphyxia-cardiac arrest rat model for developing mechanism of effect oriented therapeutic concepts after cardiopulmonary resuscitation]. *Anaesthesiol. Reanim.* **26**, 159–165 (2001).
32. Callaway, C. W. & Logue, E. S. in *Animal Models of Acute Neurological Injuries* (eds Chen, J., Xu, Z. C., Xu, X.-M. & Zhang, J. H.) 87–101 (Humana Press, 2009).
33. Hardziyenka, M., Campian, M. E., Rianne de Bruin-Bon, H. A. C. M., Michel, M. C. & Tan, H. L. Sequence of echocardiographic changes during development of right ventricular failure in rat. *J. Am. Soc. Echocardiogr.* **19**, 1272–1279 (2006).
34. Teichholz, L. E., Kreulen, T., Herman, M. V. & Gorlin, R. Problems in echocardiographic volume determinations: echocardiographic-angiographic correlations in the presence or absence of asynergy. *Am. J. Cardiol.* **37**, 7–11 (1976).
35. Watson, L. E., Sheth, M., Denyer, R. F. & Dostal, D. E. Baseline echocardiographic values for adult male rats. *J. Am. Soc. Echocardiogr.* **17**, 161–167 (2004).
36. Hocking, K. M. et al. Peripheral I.V. analysis (PIVA) of venous waveforms for volume assessment in patients undergoing haemodialysis. *Br. J. Anaesth.* **119**, 1135–1140 (2017).
37. Hanley, J. A. & McNeil, B. J. A method of comparing the areas under receiver operating characteristic curves derived from the same cases. *Radiology* **148**, 839–843 (1983).
38. Gilpin, A. R. Table for conversion of Kendall's tau to Spearman's rho within the context of measures of magnitude of effect for meta-analysis. *Educ. Psychol. Meas.* **53**, 87–92 (1993).

AUTHOR CONTRIBUTIONS

R.J.L.: data collection, analysis, and presentation; manuscript writing. M.B.B.: data collection, analysis, and presentation; manuscript writing. C.B.: study design; data collection and analysis; manuscript review. F.J.B.: study design; data collection, analysis, and presentation; manuscript review. M.L.R.: study design; data analysis and presentation; manuscript review. G.S.: data analysis and presentation; manuscript review. A.H.: data collection, analysis, and presentation; manuscript writing. S.S.E.: study design; data collection and analysis; manuscript writing. All authors read and approved the final version of the manuscript.

FUNDING

C.B. was funded by the Deutsche Forschungsgemeinschaft (DFG, German Research Foundation) – Project number BA 6287/1-1. M.B.B. was funded by the Training in Perioperative Science Award [grant number 5T32 GM108554] from the National Institutes of Health and by a starter grant from the Society of Cardiovascular Anesthesiologists. Additional support was provided by institutional funds, NIH grant (5R01 HL123227), and a Merit Review Award (I01 BX003482) from the U.S. Department of Veterans Affairs Biomedical Laboratory R&D Service awarded to M.L.R.

COMPETING INTERESTS

The authors declare no competing interests.

ADDITIONAL INFORMATION

Correspondence and requests for materials should be addressed to Ryan J. Lefevre.

Reprints and permission information is available at <http://www.nature.com/reprints>

Publisher's note Springer Nature remains neutral with regard to jurisdictional claims in published maps and institutional affiliations.

Springer Nature or its licensor holds exclusive rights to this article under a publishing agreement with the author(s) or other rightsholder(s); author self-archiving of the accepted manuscript version of this article is solely governed by the terms of such publishing agreement and applicable law.